

Supplementary Material

Simultaneous magnetic purification and detection of transferrin in human serum using an imprinting-based fluorescence sensor by boronate affinity and secondary signal amplification assay

Yuanxia Xu^a, Yanqiao Zhu^a, Jinyu Cao^a, Yanting Wang^a, Xueping Hu^{a, *}, Xiaohua Zhao^b,
*, Xingliang Song^{a, *} and Lingxin Chen^c

^aSchool of Chemistry and Chemical Engineering, Linyi University, Linyi 276000, P.R. China

^bLinyi People's Hospital, Linyi 276000, P.R. China

^cCAS Key Laboratory of Coastal Environmental Processes and Ecological Remediation, Research Center for Coastal Environmental Engineering and Technology, Yantai Institute of Coastal Zone Research, Chinese Academy of Sciences, Yantai 264003, P.R. China

*Corresponding author.

Xueping Hu

Telephone: +86 0539-7258620

Fax: +86 0539-7258620

E-mail: xuephu@yeah.net (X. Hu)

S1. Experimental

S1.1 Preparation of Fe₃O₄-NH₂@MIPs and Fe₃O₄-NH₂@NIPs

Fe₃O₄-NH₂@MIPs were prepared by the following procedure. The template layer was constructed by dispersing 100 mg Fe₃O₄-NH₂ in phosphate buffer solution (pH 7.4), and 0.8 mg/mL TRF was added to form a template layer by incubating it at room temperature overnight. Subsequently, 50 mg dopamine hydrochloride and 50 mg APS were added and reacted under continuous stirring for 3 h to form an imprinting layer encapsulated with TRF. The template was removed using 0.1 mol/L HAc containing 10% SDS. For comparison, non-imprinted polymers (Fe₃O₄-NH₂@NIPs) were also prepared under the same conditions without immobilizing the template.

S1.2 Adsorption thermodynamics

For each set of adsorption isotherm experiment, 3 mL of TRF solution with known initial concentration, C_0 (mg/mL), was mixed with 8 mg of MIPs/NIPs and agitated in an oscillator at 200 rpm for 30 minutes at 288, 298, or 308 K. The equilibrium concentration, C_e (mg/mL), of TRF in the solution was determined on a UV-vis spectrophotometer at 280 nm. Equilibrium adsorption capacity Q_e (mg/g) was calculated by:

$$Q_e = \frac{(C_0 - C_e)V}{m} \quad \#(1)$$

Where V (mL) is the volume of the solution, and m (g) is the dry weight of MIPs/NIPs.

Langmuir and Freundlich models given by the following equations were used to fit the experimental data:

Langmuir equation:

$$Q_e = \frac{Q_m K_L C_e}{1 + K_L C_e} \#(2)$$

Freundlich equation:

$$Q_e = K_F C_e^{1/n} \#(3)$$

where Q_m (mg/g) is the maximum monolayer adsorption capacity, K_L (mL/mg) is the Langmuir constant related to the adsorption energy. K_F ((mg/g)(mL/mg)^{1/n}) and 1/n are the Freundlich constants indicating the adsorption capacity and intensity, respectively.

S1.3 Adsorption kinetics

Shake centrifuge tubes containing 8mg MIPs/NIPs and 3 mL 0.3 mg/mL TRF solution in each were shaken at 200 rpm and 298 K for 2, 5, 10, 20, 40, 60, 70, and 80 min. The concentration of the TRF in the liquid phase at time t, C_t (mg/mL), was analyzed, and Q_t (mg/g), adsorption capacity at t was calculated using:

$$Q_t = \frac{(C_0 - C_t)V}{m} \#(4)$$

Pseudo-first-order and pseudo-second-order adsorption kinetic models were used in the forms as follows to fit the experimental kinetic data:

Pseudo-first-order equation:

$$Q_t = Q_e(1 - e^{-k_1 t}) \#(5)$$

Pseudo-second-order equation:

$$Q_t = \frac{t k_2 Q_e^2}{t k_2 Q_e + 1} \#(6)$$

where Q_e (mg/g) is the calculated equilibrium adsorption capacity, k_1 (1/min) and k_2 (g/(mg·min)) are the adsorption rate constants of the pseudo-first-order equation and pseudo-second-order equation, respectively.

S1.4 Selectivity experiments

The selectivity of MIPs and NIPs was assayed using OVA (ovalbumin), HRP (horseradish peroxidase), Hb (bovine haemoglobin) and BSA (bovine serum albumin) solutions. Recombinant transferrin (Re-TRF) was used to assess whether the sensor could evaluate TRFs with different degrees of glycosylation. The equilibrium concentration C_e (mg/mL) of the relevant proteins (0.2 mg/mL each) in solution was determined by UV-Vis spectrophotometer, and the equilibrium adsorption capacity Q_e (mg/g) was calculated. At the same time, MIPs and NIPs (2.5 mg/mL each) were added to 1.0 mL of correlated protein solution, and MIPs-TRF-TCPP-BA was constructed by combining with TCPP-BA after oscillation for 30 min. the fluorescence properties were then quantified using $F-F_0$. The specificity of MIPs for TRF was evaluated using the imprinting factor (IF). The IF depends on the following equation

$$IF = \frac{Q_{MIPs}}{Q_{NIPs}} = \frac{(F - F_0)_{MIPs}}{(F - F_0)_{NIPs}} \quad \#(7)$$

where Q_{MIPs} and Q_{NIPs} (mg/g) represent the adsorption capacities of template and non-template on MIPs and NIPs, respectively, while $(F - F_0)_{MIPs}$ and $(F - F_0)_{NIPs}$ represent the fluorescence difference between template and non-template on MIPs and NIPs, respectively.

S1.5 Interference Experiments

Interference experiments were performed to investigate how some anions and biomolecules commonly found in biological fluids affect MIPs-TRF-TCPP-BA.

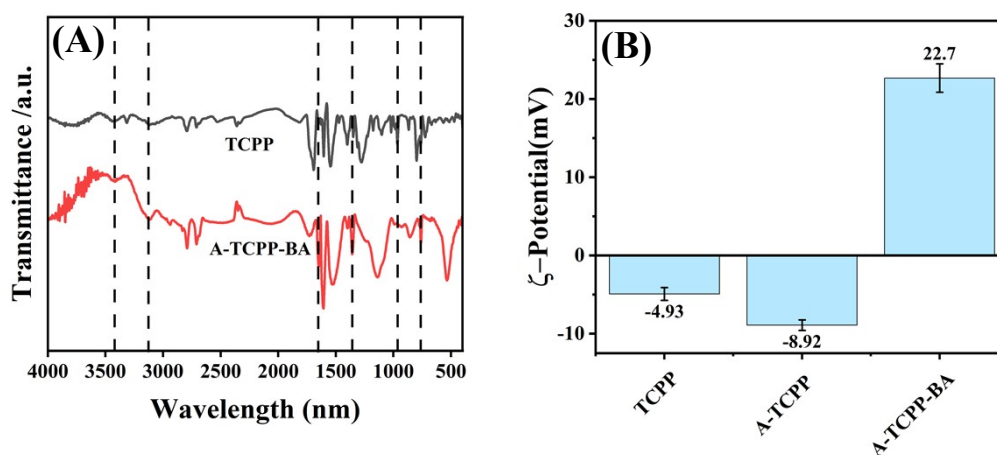
S1.6 Reusability and repeatability of MIPs

The adsorption amount Q_e was examined as an assessment of the reusability and reproducibility of MIPs-TRF. Firstly, for reusability, MIPs (8.0 mg) were dispersed in TRF (0.30 mg/mL, 3.0 mL) solution and shaken for 30 min. The supernatant was taken

after magnetic separation and the equilibrium concentration C_e (mg/mL) of TRF in solution, was determined by UV-Vis spectrophotometer at 280 nm, and the equilibrium adsorption capacity Q_e (mg/g) was calculated. The TRF adsorbed on the material was then removed with 0.1 M acetic acid buffer containing 10% sodium dodecyl sulfate. Seven adsorption and elution cycles were operated and the adsorbed amount Q_e (mg/g) was recorded and compared. Four batches of MIPs were subsequently prepared using the same procedure and the above evaluation was repeated to examine the reproducibility of the material.

The fluorescence values were examined to assess the reproducibility and repeatability of MIPs-TRF-TCPP-BA. Firstly, for the reusability, 50 mg of MIPs/NIPs were weighed and dispersed in 10 mL of water, and 1 ml of the above dispersion was added to the TRF solution to form MIPs-TRF, and then a solution of A-TCPP-BA was used to label the TRF to form the sandwich structure of the sensor MIPs-TRF-TCPP-BA, and the A-TCPP-BA was decomposed to produce the fluorescence signals by adding the sodium hydroxide solution with a pH 10. A-TCPP-BA was decomposed by adding sodium hydroxide solution with pH 10 to generate fluorescent signals. After magnetic separation, the excitation wavelength of the supernatant was measured at 370 nm. The TRF adsorbed on the material was then removed with 0.1 M acetate buffer containing 10% sodium dodecyl sulfate. Seven adsorption and elution cycles were performed, and the fluorescence values were recorded and compared. Four batches of MIPs were subsequently prepared using the same procedure, which was repeated to evaluate the reproducibility of the material.

S2. Results and discussion



S2.1 Characterization of the prepared materials

Fig. S1. (A) FTIR spectra of TCP and A-TCP-BA; (B) Zeta potential changes during A-TCP-BA synthesis.

Fig. S1A shows the FT-IR spectra of TCP and A-TCP-BA. The ones at 761 cm^{-1} and 3120 cm^{-1} indicate the pyrrole ring=C-H absorption peak and C-H vibration on the pyrrole ring, respectively. The results at 963 cm^{-1} , 1650 cm^{-1} and 3316 cm^{-1} are attributed to the bending vibration of the N-H of the amino group, the C=O stretching vibration of the amide bond and the stretching vibration of the N-H of the amino group, respectively, which indicate the successful preparation of the boronic acidated porphyrin molecule.

Fig. S1B shows the zeta potential characterization of TCP, A-TCP, and A-TCP-BA. The absolute value of the potential of A-TCP becomes larger compared with that of TCP, indicating that the whole system tends to be stable. A-TCP produce unstable amino-active O-acyl urea intermediates through carboxyl group activation, which reacts with NHS to produce amino-active NHS esters, and then substitution with m-

aminophenylboronic acid to form amide bonds. The potential of A-TCPP-BA is positive, indicating that the amino-active NHS ester has a positive effect on the negative charge.

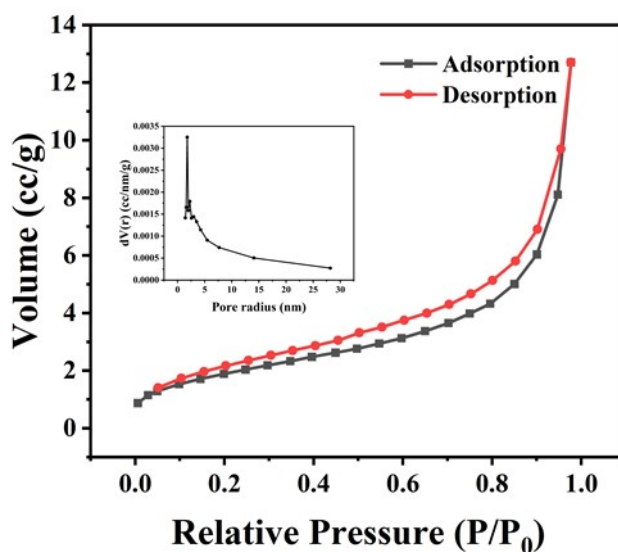


Fig. S2. N₂ adsorption-desorption isotherms of MIPs

Table S1 The surface area, pore volume, and pore radius of the MIPs and NIPs

Content	Surface Area (m ² /g)	Pore Volume (cc/g)	Pore radius Dv (nm)
MIPs	14.682	0.029	1.777
NIPs	6.934	0.018	1.778

S2.2 Adsorption performance

The equilibrium adsorption data of TRF on MIPs (NIPs) were fitted with Langmuir and Freundlich adsorption models:

Langmuir equation:

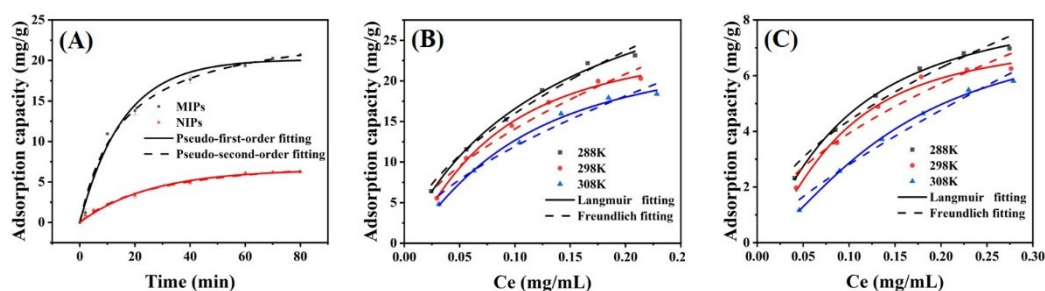
$$Q_e = \frac{Q_m K_L C_e}{1 + K_L C_e} \quad \#(8)$$

Freundlich equation:

$$Q_e = K_F C_e^{\frac{1}{n}} \quad \#(9)$$

where Q_m (mg/g) is the maximum monolayer adsorption capacity, K_L (mL/mg) is

the Langmuir constant related to the adsorption energy. K_F ((mg/g)(mL/mg)^{1/n}) and 1/n are the Freundlich constants indicating the adsorption capacity and intensity,



respectively, n denotes the inhomogeneity of the adsorbent surface and the favourable degree of adsorption.

Fig. S3 (A) Adsorption kinetics of MIPs and NIPs for TRF detection at 298 K. Adsorption isotherms of MIPs (B) and NIPs (C) on TRF at 288, 298 and 308 K.

Table S2 Parameters from Langmuir and Freundlich models for the adsorption isotherms of TRF on MIPs and NIPs

Adsorbent	Temperature(K)	Langmuir			Freundlich		
		Q_{max} (mg/g)	K_L (mg/g)	R^2	K_F (mg/g)	$1/n$	R^2
MIPs	288	41.725	5.641	0.994	58.999	0.566	0.985
	298	26.150	28.868	0.996	51.803	0.565	0.964
	308	25.459	18.993	0.993	48.195	0.606	0.968
NIPs	288	8.946	19.937	0.997	14.507	0.519	0.964
	298	7.468	47.147	0.988	13.581	0.538	0.932
	308	8.178	17.823	0.998	16.0276	0.763	0.976

Table S3 Adsorption thermodynamic parameters of TRF by MIPs and NIPs

Adsorbent	ΔG (kJ/mol)			ΔH^0 (kJ/mol)	ΔS (J/mol K)
	288 K	298 K	308 K		

MIPs	-13.413	-13.358	-13.186	-18.467	-17.460
NIPs	-9.974	-9.897	-9.011	-36.300	-88.60

The free energy of adsorption (ΔG), enthalpy of adsorption (ΔH^0) and entropy of adsorption (ΔS) of TRF on MIPs (NIPs) were calculated based on the adsorption isotherms of the two adsorbents at different temperatures by applying Van Hoff's equation, and their values are summarized in Table S3. The negative ΔG values of TRF at the three temperatures reveal the thermodynamic spontaneous nature of the adsorption of TRF on MIPs (NIPs), and the small changes in ΔG values with temperature for both analytes indicate thermo-entropic compensation during the adsorption process. The negative ΔS values of TRF on MIPs (NIPs) indicate the decrease of stoichiometry between the interfaces of adsorbed solutions during the adsorption process. The negative ΔH^0 values of TRF on MIPs (NIPs) indicate that the adsorption of TRF on MIPs (NIPs) is an exothermic process. In addition, both negative ΔS and ΔH^0 values indicate that the adsorption of TRF on MIPs (NIPs) is thermally driven^{1,2}.

In addition, adsorption kinetic data for both adsorbents were analysed using pseudo-first-order and pseudo-second-order kinetic models:

Pseudo-first-order equation:

$$Q_t = Q_e(1 - e^{-k_1 t}) \quad \#(10)$$

Pseudo-second-order equation:

$$Q_t = \frac{tk_2 Q_e^2}{tk_2 Q_e + 1} \quad \#(11)$$

where Q_e (mg/g) is the calculated equilibrium adsorption capacity, and k_1 (1/min) and k_2 (g/ (mg·min)) are the adsorption rate constants for the pseudo-first-order and pseudo-second-order equations, respectively.

The calculated values of k_1 , k_2 and Q_e and the correlation coefficient r^2 are summarized in Table S4.

As can be seen from the table S4, the pseudo-second-order kinetic model fits the kinetic data well for both MIPs and NIPs. Based on the assumptions of the pseudo-

second-order kinetic model, it was confirmed that the adsorption of TRF on MIPs and NIPs was chemisorbed and exhibited a reversible covalent reaction between boric acid and TRF, which is consistent with what was previously reported by He et al., and that this is the primary mechanism for the recognition of boronate affinity.

Table S4 Parameters from Pseudo-first-order and Pseudo-second-order models for the adsorption kinetics of TRF on MIPs and NIPs at 298 K

Adsorbent	$Q_{e,exp}$ (mg/g)	Pseudo-first-order fitting			Pseudo-second-order fitting		
		$Q_{e,cal}$ (mg/g)	k_1	r^2	$Q_{e,cal}$ (mg/g)	k_2	r^2
MIPs	20.704	20.136	0.0636	0.989	24.603	0.00265	0.992
NIPs	6.263	6.558	0.0388	0.990	8.622	0.00407	0.993

To confirm the role of boronate affinity in TRF recognition, control experiments were conducted using imprinted and non-imprinted polymers synthesized without boronate chemistry. The results are shown in Table S5, it can be seen that the adsorption capacity of the imprinted polymer after boronate functionalization (MIPs) is significantly higher than that of the material without boronate functionalization ($Fe_3O_4-NH_2@MIPs$). The above results also further proved that the interaction between the imprinted polymers and transferrin is boronate chemistry. In addition, although in the "sandwich" structure design, the fluorescent tag uses the same chemistry (boronate) to bound to transferrin. However, due to the use of signal amplification strategy in the detection process, the proposed method still shows high detection sensitivity.

Table S5 Results of the adsorption capacity of MIPs, NIPs, $Fe_3O_4-NH_2@MIPs$ and $Fe_3O_4-NH_2@NIPs$

Materials	Q_e (mg/g)
MIPs	20.704
NIPs	6.263
$Fe_3O_4-NH_2@MIPs$	3.642

S2.3 Analytical performance of NIPs-TRF-TCPP-BA sensor

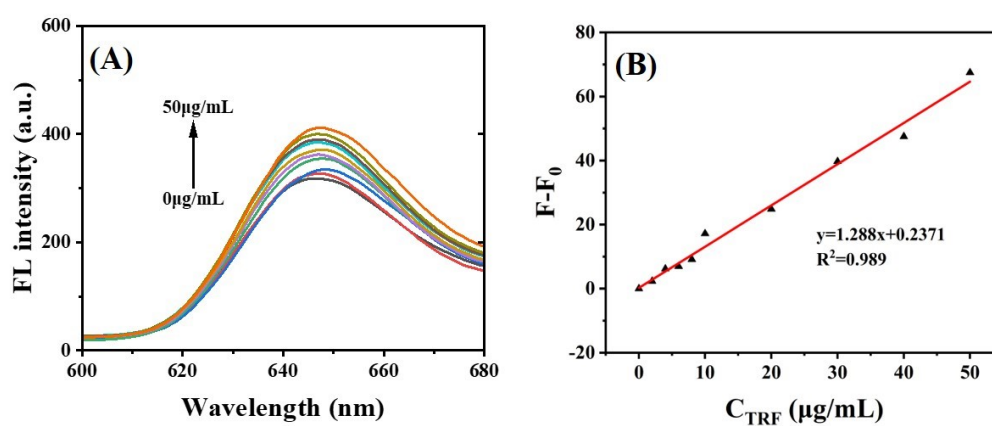
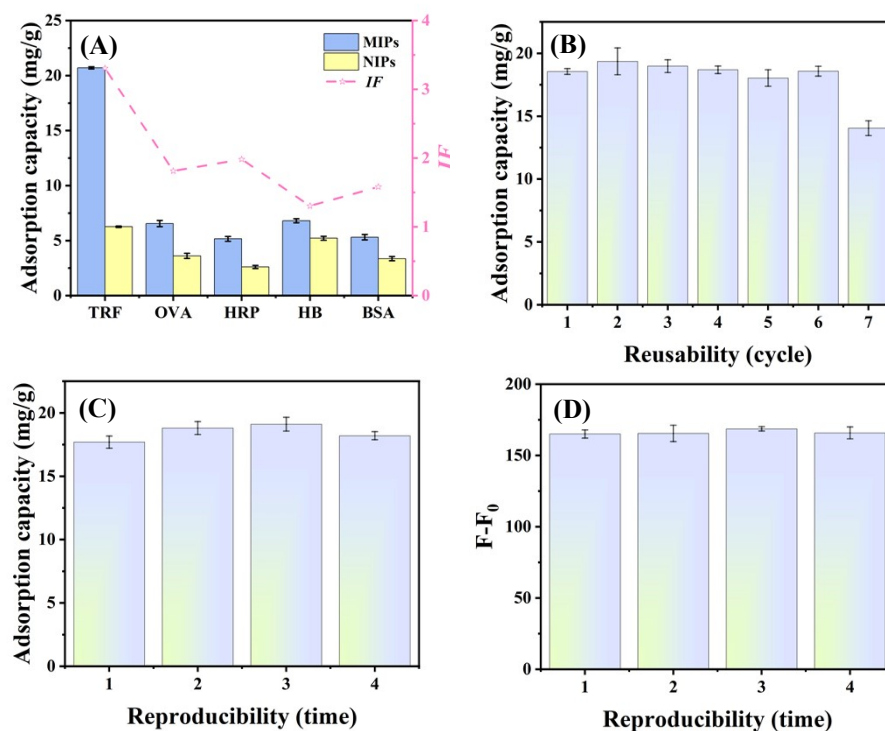


Fig. S4. (A) Fluorescence spectra of the NIPs-TRF-TCPP-BA sensor at a series of TRF concentrations and (B) linear fit to the corresponding concentrations

S2.4 Selectivity and Reproducibility and Reusability of MIPs-TRF



and MIPs-TRF-TCPP-BA

Fig. S5. (A) Adsorption selectivity of MIPs/NIPs; (B) Reproducibility of MIPs-TRF (different batches, Adsorption as a comparison); (C) Reusability of MIPs-TRF (same batches); (D) Reproducibility of MIPs (different batches, Fluorescence values as a comparison)

The adsorption amount Q_e was examined as a means of assessing the reusability and reproducibility of MIPs-TRFs. Firstly, we examined the reproducibility. The MIPs-TRF was constructed and the equilibrium adsorption capacity Q_e (mg/g) of MIPs with adsorbed TRF was calculated, after which the TRF adsorbed on the material was removed with 0.1 M acetic acid buffer containing 10% sodium dodecyl sulfate. Seven adsorption and elution cycles were operated. Secondly, we examined the reusability. As shown in Fig. S5C, four batches of MIPs were prepared using the same steps and the above steps were repeated. As shown in Fig. S5B, MIPs could be used for six replicate experiments with less than 10% reduction in adsorption. This result shows that the MIPs can be reused and meet practical testing requirements, and the material

has good reproducibility.

Table S6 Results of the adsorption capacity and fluorescence signals of TRF and Re-TRF

Absorbent	Qe(mg/g)	F-F ₀
TRF	20.704	167.009
Re-TRF	9.909	91.864

The adsorption capacity as well as fluorescence signals of recombinant transferrin are shown in the Table S6. It can be seen that the sensor can distinguish between TRFs with different degrees of glycosylation, which is expected to expand the potential applications in diseases related to altered glycosylation of TRFs.

S2.5 Real sample

Table S7 TRF levels in serum samples of male/female of different age groups

Sample (male)	Concentration of TRF in human serum ($\mu\text{g}/\text{mL} \pm \text{RSD}, n=3$)	Sample (female)	Concentration of TRF in human serum ($\mu\text{g}/\text{mL} \pm \text{RSD}, n=3$)
1(0~10 years old)	3283.17 \pm 0.02	11(0~10 years old)	2918.92 \pm 0.11
2(10~20 years old)	3264.74 \pm 0.04	12(10~20 years old)	2408.69 \pm 0.07
3(20~30 years old)	2366.29 \pm 0.08	13(20~30 years old)	2351.05 \pm 0.04
4(30~40 years old)	2540.20 \pm 0.06	14(30~40 years old)	2624.73 \pm 0.03
5(40~50 years old)	2337.85 \pm 0.10	15(40~50 years old)	2195.56 \pm 0.05
6(50~60 years old)	2390.70 \pm 0.05	16(50~60 years old)	2515.96 \pm 0.06
7(60~70 years old)	2463.47 \pm 0.03	17(60~70 years old)	2500.73 \pm 0.03
8(70~80 years old)	2745.72 \pm 0.01	18(70~80 years old)	2323.91 \pm 0.04
9(80~90 years old)	2979.43 \pm 0.04	19(80~90 years old)	2785.90 \pm 0.06

10(90~100 years old)	3120.30 ± 0.07	20(90~100 years old)	2641.74 ± 0.05
----------------------	--------------------	----------------------	--------------------

The TRF content is monitored in the serum of male and female of different age groups; 1~10 are male and 11~20 are female samples. The TRF content in male samples in the same age group exceeds females in the same age group (Table S7). At the same time, the TRF content of male and female samples shows the distribution of "two ends high and middle-low", where TRF levels in serum are higher in older and younger age groups than in intermediate age groups. The above results indicate that the MIPs-TRF-TCPP-BA sensor exhibits good application prospects, with good accuracy for TRF detection, and can be further used as a tool for biomarker detection in certain diseases.

S3. References

1. Y. Li, M. Cheng, Y. Jiang, G. Pan, H. Wang and S. Shan, *Journal of Inorganic and Organometallic Polymers and Materials*, 2019, 30, 2551-2561.
2. Y. Li, F. M. Hagos, R. Chen, H. Qian, C. Mo, J. Di, X. Gai, R. Yang, G. Pan and S. Shan, *Bioresources and Bioprocessing*, 2021, 8.